

Mathematical Modelling and Attitude Control of Quadcopter based on Classical Controller

S. Senthil Kumar^{a,b}, R. Vijayanandh^{a,c} and S. Mano^d

^aDept. of Aeronautical Engg., Kumaraguru College of Tech., Coimbatore, India

^bCorresponding Author, Email: senthil.avionics@gmail.com

^cEmail: vijayanandh.raja@gmail.com

^dSchool of Mechanical Engg., SASTRA Deemed University, Tanjore, India
Email: mano.aeronz@gmail.com

ABSTRACT:

The development of vertical take-off and landing (VTOL) aircrafts has been increasing in recent years due to growing demands in various sectors for critical missions and time saving purpose. There are number of configurations exist for VTOL airframe such as single-main-rotor, tandem rotor, coaxial rotor, tri-rotor, quad-rotor and hexa-rotor. Among various configurations quad-rotor and hexa-rotor configurations have been chosen frequently for various applications through miniature aircrafts. The components and subsystems of such configurations have been widely available for easy integration and flight tests. In addition to that, classical control methods such as proportional-integral-derivative (PID) controllers have been widely employed for better control of such aircrafts with stable operation. Even though the control methods are available with high performance flight controller boards, the attainment of quicker attitude response and better stability will be a major problem during the flight testing phase for quadcopters and hexacopters. Therefore, instead of directly going into the development of quadcopters, there should be a need for simulating their responses with models of actual configuration. In this paper, a quadcopter dynamics for roll, pitch, and yaw have been modelled as mathematical equations and its response have been simulated in MATLAB using classical control tools. The results have shown that the modelled dynamics respond faster with better stability.

KEYWORDS:

Quadcopter; Dynamic response; Stability analysis; Classical control; MATLAB

CITATION:

S. Senthil Kumar, R. Vijayanandh and S. Mano. 2018. Mathematical Modelling and Attitude Control of Quadcopter based on Classical Controller, *Int. J. Vehicle Structures & Systems*, 10(5), 318-323. doi:10.4273/ijvss.10.5.02.

ACRONYMS AND NOMENCLATURE:

Φ	Roll angle (deg or rad)
Θ	Pitch angle (deg or rad)
Ψ	Yaw angle (deg or rad)
x,y,z	Linear position of quadcopter (m)
u,v,w	Linear velocities of quadcopter (m/s)
p	Body roll rate (deg/s or rad/s)
q	Body pitch rate (deg/s or rad/s)
r	Body yaw rate (deg/s or rad/s)
R	Rotation matrix from body frame to inertial frame
f_i	Force in the direction of rotor axis
τ_{M_i}	Torque around rotor axis
k	Lift constant
b	Drag constant
g	Acceleration due to gravity (m/s ²)

1. Introduction

The use of unmanned aerial vehicles (UAVs), or drones, has many interesting applications. Beyond the uses within military applications, UAVs can perform search and rescue operations in hazardous environments, surveillance and inspections of hard to reach places. UAVs can even be used for acrobatic aerial footage in the film making industry or in the future for home

delivery of purchased goods. One type of an UAV is a multicopter that is equipped with a control system. This is an agile, flying platform that can be modified in size and capabilities for whatever application the designer has in mind. A multicopter is the designation of a rotorcraft with more than two rotors and a quadcopter is the designation for the special case of four rotors. The goal of quad-rotor designers is to remove rotor-head control systems applying both cyclic and collective pitch changes to the rotor blades as the means of aircraft control. The idea is to have the rotor blades all fixed in pitch and to achieve thrust changes on each rotor by changing its speed of rotation.

Each rotor is individually driven by an electric motor mounted at the rotor head. Thus, for example, for the aircraft to move forward the rotational speed of the two rear rotors would be increased to pitch the aircraft nose-down and direct the resulting thrust vector forwards. At the same time the total thrust must be increased to prevent loss of height and, once established in forward flight, the rotor speeds must again be harmonized. The control algorithms to achieve this are extremely complicated, taking into account also the changing aerodynamic interference patterns between the rotors. There must be a time-lag in the demanded speed

change of each rotor although this becomes less of a problem with the low inertias of a small micro aerial vehicle (MAV). The configuration is naturally more gust-sensitive than the other configurations, and its control response must be expected to be slower. Therefore the achievement of adequate control may be difficult enough in the still air of laboratory conditions and even more problematic in the turbulent air of urban operations.

Power failures, either of any one of the individual motors or of the power supply, may be considered unlikely, but such an event would spell an immediate uncontrolled descent to earth. For controlling the quadcopters in flight, gyroscopes and accelerometers are traditional ways of implementing attitude control and still used in many systems. In more recent systems there is an increased tendency to use ‘strapped down’ sensors fixed to the body axes. These directly provide body rates for control, but need mathematical integration to give attitude and heading as undertaken within inertial navigation systems. The functions of the control and stability of a quadcopter will depend in nature on the different aircraft configurations and the characteristics required of them. Quadcopter has received considerable attention from researchers as the complex phenomena of the quadcopter have generated several areas of interest.

The basic dynamical model of the quadcopter is the starting point for all of the studies but more complex aerodynamic properties has been introduced as well. The dynamics of quadcopter can be obtained using liberalized equations of motion for the purpose of simulating the response of the aircraft for attitude inputs with suitable controllers. Once the simulated response is satisfied, we could achieve a better control in real-time flight with the designed controller gains using software. A typical control loop for attitude control of quadcopter is shown in Fig. 1. Different control methods have been researched, including proportional-integral-derivative (PID) controllers and various non-linear control methods. Here, the stabilization of the quadcopter is conducted by utilizing a classical controller.

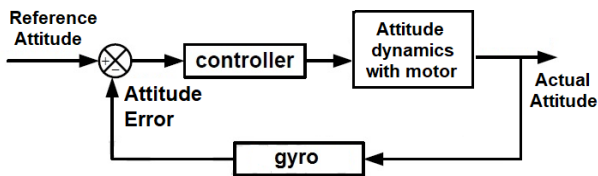


Fig. 1: Control loop for attitude control of quadcopter

2. Modelling of quadcopter dynamics

The differential equations of the quadcopter dynamics have been presented. They are derived from Newton-Euler equations which are used in the study of quadcopters. The behavior of the model is examined by simulating the flight of the quadcopter. The quadcopter structure is presented in Fig. 2 including the corresponding angular velocities, torques and forces created by the four rotors (numbered from 1 to 4). The absolute linear position of the quadcopter is defined in the inertial frame x, y, z axes with ξ the attitude (angular position) is defined in the inertial frame with

three Euler angles η . Pitch angle θ determines the rotation of the quadcopter about the y -axis, roll angle ϕ determines the rotation about the x -axis and yaw angle ψ determines the rotation about the z -axis.

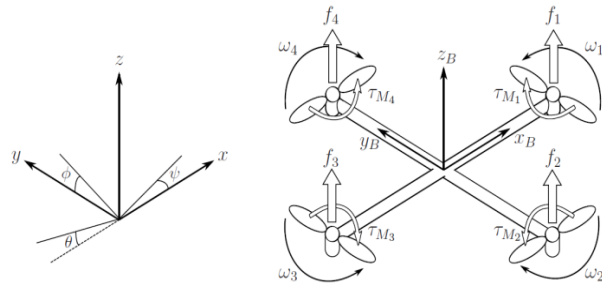


Fig. 2: Inertial and body frames of a quadcopter

Vector Q contains the linear and angular position vectors as follows,

$$\xi = \begin{bmatrix} x \\ y \\ z \end{bmatrix} \quad \eta = \begin{bmatrix} \phi \\ \theta \\ \psi \end{bmatrix} \quad Q = \begin{bmatrix} \xi \\ \eta \end{bmatrix} \quad (1)$$

The origin of the body frame is in the center of mass of the quadcopter. In the body frame, the linear velocities are determined by L and the angular velocities are determined by ω :

$$L = \begin{bmatrix} u \\ v \\ w \end{bmatrix}; \quad \omega = \begin{bmatrix} p \\ q \\ r \end{bmatrix} \quad (2)$$

The rotation matrix from the body frame to the inertial frame is given by:

$$R = \begin{bmatrix} c\theta c\psi & s\phi s\theta c\psi - c\phi s\psi & c\phi s\theta c\psi + s\phi s\psi \\ c\theta s\psi & s\phi s\theta s\psi + c\phi c\psi & c\phi s\theta s\psi - s\phi c\psi \\ -s\theta & s\phi c\theta & c\phi c\theta \end{bmatrix} \quad (3)$$

Where c and s are cosine and sine functions. The rotation matrix R is orthogonal thus $R^{-1} = R^T$ which is the rotation matrix from the inertial frame to the body frame. The Euler rates $\dot{\eta}$ and body rates ω are related by,

$$\begin{bmatrix} \dot{\phi} \\ \dot{\theta} \\ \dot{\psi} \end{bmatrix} = \begin{bmatrix} 1 & \sin\phi \tan\theta & \cos\phi \tan\theta \\ 0 & \cos\phi & -\sin\phi \\ 0 & \sin\phi \sec\theta & \cos\phi \sec\theta \end{bmatrix} \begin{bmatrix} p \\ q \\ r \end{bmatrix} \quad (4)$$

The quadcopter is assumed to have symmetric structure with the four arms aligned with the body x and y axes. Thus, the inertia matrix is diagonal matrix I in which

$$I_{xx} = I_{yy}$$

$$I = \begin{bmatrix} I_{xx} & 0 & 0 \\ 0 & I_{yy} & 0 \\ 0 & 0 & I_{zz} \end{bmatrix} \quad (5)$$

The angular velocity of rotor i , denoted with ω_i , create force f_i in the direction of the rotor axis. The angular velocity and acceleration of the rotor also create torque τ_{M_i} around the rotor axis using,

$$f_i = k\omega_i^2, \quad \tau_{M_i} = b\omega_i^2 + I_M\dot{\omega}_i \quad (6)$$

In which the lift constant is k , the drag constant is b and the moment of inertia of the rotor is I_M . Usually the effect $\dot{\omega}_i$ is considered small and thus it is omitted.

The combined forces of rotors create thrust T in the direction of the body z axis. Torque τ_B consists of the torques τ_ϕ, τ_θ and τ_ψ in the direction of the corresponding body frame angles

$$T = \sum_{i=1}^4 f_i = k \sum_{i=1}^4 \omega_i^2; T^B = \begin{bmatrix} 0 \\ 0 \\ T \end{bmatrix} \quad (7)$$

$$\tau_B = \begin{bmatrix} \tau_\phi \\ \tau_\theta \\ \tau_\psi \end{bmatrix} = \begin{bmatrix} l k (-\omega_2^2 + \omega_4^2) \\ l k (-\omega_1^2 + \omega_3^2) \\ \sum_{i=1}^4 \tau_{Mi} \end{bmatrix} \quad (8)$$

In which l is the distance between the rotor and the centre of mass of the quadcopter. Thus, the roll movement is acquired by decreasing the 2nd rotor velocity and increasing the 4th rotor velocity. Similarly, the pitch movement is acquired by decreasing the 1st rotor velocity and increasing the 3rd rotor velocity. Yaw movement is acquired by increasing the angular velocities of two opposite rotors and decreasing the velocities of the other two.

2.1. Newton-Euler equations

The quadcopter is assumed to be rigid body and thus Newton-Euler equations can be used to describe its dynamics. In the body frame, the force required for the acceleration of mass $m\dot{L}$ and the centrifugal force $\omega \times (mL)$ are equal to the gravity $R^T G$ and the total thrust of the rotors T_B .

$$m\dot{L} + \omega \times (mL) = R^T G + T_B \quad (9)$$

In the inertial frame, the centrifugal force is nullified. Thus, only the gravitational force and the magnitude and direction of the thrust are contributing in the acceleration of the quadcopter,

$$m\ddot{\xi} = G + R T_B \quad (10)$$

$$\begin{bmatrix} \ddot{x} \\ \ddot{y} \\ \ddot{z} \end{bmatrix} = \begin{bmatrix} 0 \\ 0 \\ -g \end{bmatrix} + \frac{T}{m} \begin{bmatrix} \cos \phi \sin \theta \cos \psi + \sin \phi \sin \psi \\ \cos \phi \sin \theta \sin \psi - \sin \phi \cos \psi \\ \cos \phi \cos \theta \end{bmatrix} \quad (11)$$

In the body frame, the angular acceleration of the inertia $I\dot{\omega}$, the centripetal forces $\omega \times (I\omega)$ and the gyroscopic forces Γ are equal to the external torque τ

$$I\dot{\omega} + [\omega \times (I\omega)] + \Gamma = \tau \quad (12)$$

$$\dot{\omega} = I^{-1} \left(- \begin{bmatrix} p \\ q \\ r \end{bmatrix} \times \begin{bmatrix} I_{xx} p \\ I_{yy} q \\ I_{zz} r \end{bmatrix} - I_r \begin{bmatrix} p \\ q \\ r \end{bmatrix} \times \begin{bmatrix} 0 \\ 0 \\ 1 \end{bmatrix} \omega_\Gamma + \tau \right) \quad (13)$$

$$\begin{bmatrix} \dot{p} \\ \dot{q} \\ \dot{r} \end{bmatrix} = \begin{bmatrix} (I_{yy} - I_{zz}) qr / I_{xx} \\ (I_{zz} - I_{xx}) pr / I_{yy} \\ (I_{xx} - I_{yy}) pq / I_{zz} \end{bmatrix} - I_r \begin{bmatrix} q / I_{xx} \\ -p / I_{yy} \\ 0 \end{bmatrix} \omega_\Gamma + \begin{bmatrix} \tau_\phi / I_{xx} \\ \tau_\theta / I_{yy} \\ \tau_\psi / I_{zz} \end{bmatrix} \quad (14)$$

In which $\omega_\Gamma = \omega_1 - \omega_2 + \omega_3 - \omega_4$.

2.2. Transfer functions of attitude dynamics

The transfer functions of quadcopter attitude dynamics have been obtained using Laplace transform by assuming the quadcopter is initially in a stable state in which the

values of all positions and angles are zero, the body frame of the quadcopter is congruent with the inertial frame. The total thrust is equal to the hover thrust, the thrust equal to gravity. By selecting the motors with a bandwidth of 30 rad/s, the roll dynamics is represented by a transfer function relating the body roll rate (p) output (y_{out}) to an applied rate command (u_{ref}) and is given by,

$$\left(\frac{u_{ref}}{y_{out}} \right)_{roll\ rate} = \frac{15000}{(s+30)(s+1)} \quad (15)$$

Here, an amplification of 500 from the motor signals to angular rate, and a factor of $s+1$ corresponding to a weakly attenuated angular rate have been considered. After adding an integrator and selecting the feedback gyro gain of 1, the block diagram of roll angle dynamics have been formed and is shown in Fig. 3. Where, K is open-loop system gain. With the same motor bandwidth, an amplification of 300 from the motor signals to angular rate, a factor of $s+1$ corresponding to a weakly attenuated angular rate and a pure integration from angular rate to angle, the pitch dynamics is given by,

$$\left(\frac{u_{ref}}{y_{out}} \right)_{pitch} = \frac{9000}{s(s+30)(s+1)} \quad (16)$$

Note that the amplification is weaker than in roll. This could be because the quadcopter is longer along the x -axis than the y -axis and this causes the moment of inertia to be larger. And finally, with the same motor and an amplification of 35.7 from the motor signals to angular rate, the yaw dynamics is given by,

$$\left(\frac{u_{ref}}{y_{out}} \right)_{yaw} = \frac{750}{s(s+30)(s+0.7)} \quad (17)$$

The block diagram of pitch and yaw dynamics are similar to the one shown in Fig. 3 by considering the corresponding transfer functions of pitch and yaw as given in Eqns. (16) and (17), respectively

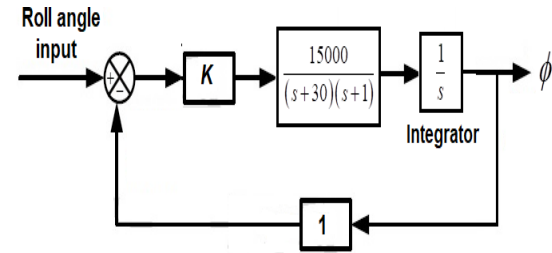


Fig. 3: Roll angle dynamics of quadcopter

3. Controller design for attitude control

In order to control the orientation of the quadcopter, an attitude controller has been implemented. The attitude controller consists of three decoupled controllers, a roll controller, a pitch controller and a yaw controller.

3.1. Roll controller

For the roll dynamics transfer functions given in Fig. 3, the root locus for the open-loop system have been obtained and is shown in Fig. 4. From the root locus, we have selected 5% overshoot in roll angle and its corresponding dominant pole is $-0.491 \pm 0.515j$ and the open-loop gain K value is 0.00101. With the obtained gain value, the response of roll angle is obtained and is shown in Fig. 5. From the roll angle response with 5% overshoot, the peak time is observed as 6.19 s, the rise

time is found as 2.96 s, and the settling time is 8.47 s. And also it is clear that the final value is settled at exactly 1, hence the steady-state error is zero. Therefore, there is no need for integral control and only PD controller is required to improve the transient response further. Here, the design specification for roll controller is to reduce the peak time to 2 s. From the second-order transient response specifications, the imaginary value of the desired dominant pole for the peak time of 2 s is found as ± 1.57 . And for the 5% overshoot, the real part of the dominant pole is obtained from trigonometry and is found as -1.5 . Therefore, the desired dominant pole for the required peak time is $-1.5 \pm 1.57j$. For the desired dominant pole, the PD controller's zero can be obtained from the root locus properties and trigonometry and is found as -2.249 .

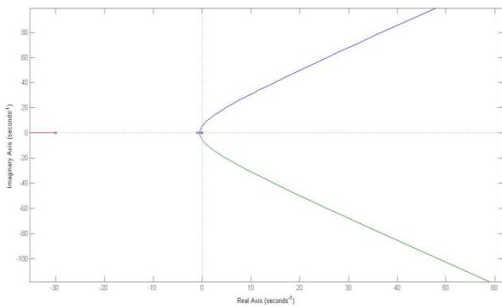


Fig. 4: Root locus for roll angle transfer function

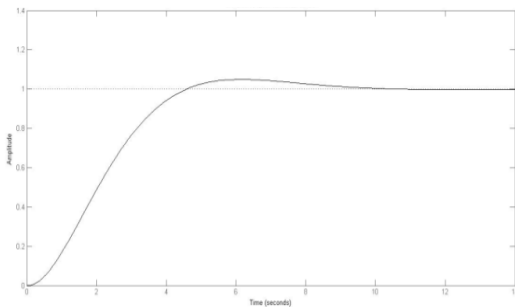


Fig. 5: Roll angle response of quadcopter without controller

Now, the open-loop gain K for the PD compensated system can be obtained by plotting the root locus for the open-loop system with the roll angle transfer function and the PD controller transfer function of $s+2.249$ and is shown in Fig. 6. From the root locus of PD compensated system, the open-loop gain K is found as 0.00389. Therefore, the final transfer function of PD roll controller is $0.00389(s+2.249)$. From that, the proportional gain (K_p) of PD controller is 0.00875 and the derivative gain (K_d) is 0.00389.

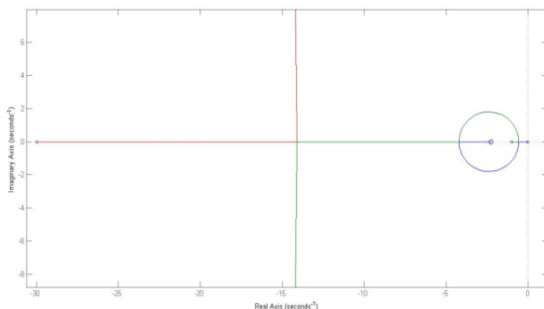


Fig. 6: Root locus for roll angle transfer function with PD controller

3.2. Pitch controller

It is noted that the denominator of pitch dynamics transfer function is same as roll dynamics. The design specification for the pitch controller is same as roll controller, i.e., peak time of 2 s and overshoot of 5%. Hence, the pitch controller design procedure is similar to the roll controller design, because the desired dominant pole is same as the one obtained in the roll controller design i.e., $-1.5 \pm 1.57j$. The PD controller transfer function for the pitch angle control is again $s+2.249$. From the root locus of PD compensated system for the pitch control, the open-loop gain K is found as 0.00648. Therefore, the final transfer function of PD pitch controller is $0.00648(s+2.249)$. From that, the proportional gain (K_p) of PD controller is 0.01457 and the derivative gain (K_d) is 0.00648.

3.3. Yaw controller

For the yaw dynamics transfer function given in Eqn. (17), the root locus for the open-loop system have been obtained and is shown in Fig. 7. From the root locus, for 5% overshoot in yaw angle and its corresponding dominant pole is $-0.346 \pm 0.363j$ and the open-loop gain K value is 0.01. With the obtained gain value, the response of yaw angle is obtained and is shown in Fig. 8. From the yaw angle response with 5% overshoot, the peak time is observed as 8.79 s, the rise time is found as 4.2 s, and the settling time is 12 s. The final value is settled at exactly 1, hence there is no need for integral control for yaw control. Therefore, PD controller has to be implemented for yaw control to improve the transient response further. Now, the design specification for yaw controller is to reduce the peak time to 1.5 s. From the second-order transient response specifications, the imaginary value of the desired dominant pole for the peak time of 1.5 s is found as ± 2.0944 . For the 5% overshoot, the real part of the dominant pole is obtained from trigonometry and is found as -2 . Therefore, the desired dominant pole for the required peak time is $-2 \pm 2.0944j$. For the desired dominant pole, the PD controller's zero can be obtained from the root locus properties and trigonometry and is found as -3.5 . The open-loop gain K for the PD compensated system can be obtained by plotting the root locus for the open-loop system with the yaw angle transfer function and the PD controller transfer function of $s+3.5$ and is found as 0.22. Therefore, the final transfer function of PD yaw controller is $0.22(s+3.5)$. From that, the proportional gain (K_p) of PD controller is 0.77 and the derivative gain (K_d) is 0.22.

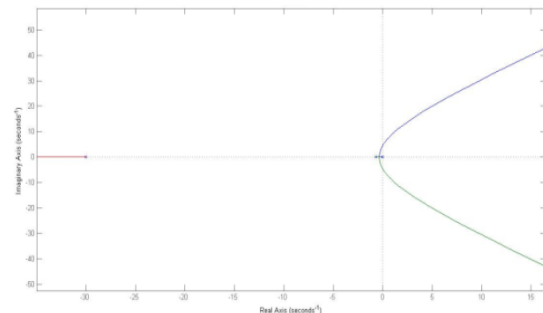


Fig. 7: Root locus for yaw angle transfer function

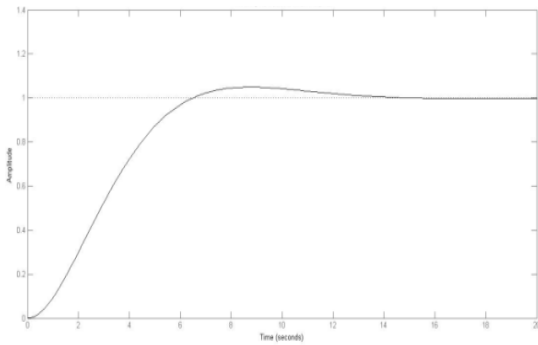


Fig. 8: Yaw angle response of quadcopter without controller

4. Simulation results

The results of MATLAB simulation for the attitude response of the quadcopter with and without controller have been discussed here. The response of the quadcopter has been compared with controller and without controller and the results have been tabulated. And the stability of the quadcopter is also verified after adding the controllers.

4.1. Roll response

It is already clear that the roll attitude response with 5% overshoot without controller have peak time of 6.19 s, rise time of 2.96 s, and settling time of 8.47 s. After adding the PD controller for roll control having the transfer function $0.00389(s+2.249)$, the response have been plotted and is compared with the roll response without controller as shown in Fig. 9. It is found that the transient response of roll attitude is improved after adding the PD controller. The results of roll response with and without controller have been given in Table 1.

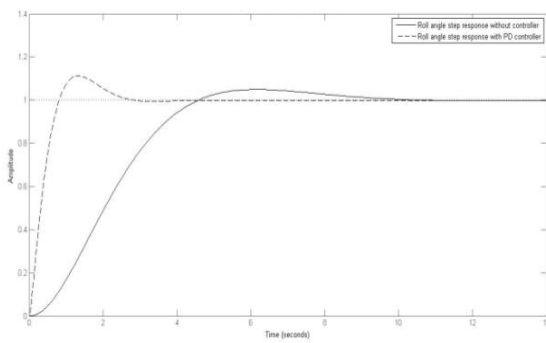


Fig. 9: Comparison of roll response with and without controller

Table 1: Performance of roll controller

Specification	Without controller	With PD controller
Rise time	2.96 s	0.577 s
Peak time	6.19 s	1.33 s
Overshoot	5%	10%
Settling time	8.47 s	2.39 s
Steady-state error	zero	zero
Closed-loop stability	stable	stable

4.2. Pitch response

The pitch attitude response with 5% overshoot without controller have peak time of 6 s, rise time of 2.95 s, and settling time of 8.46 s. After adding the PD controller for pitch control having the transfer function $0.00648(s+2.249)$, the response have been plotted and is compared with the pitch response without controller as shown in Fig. 10. It is found that the transient response of pitch attitude is further improved after adding the PD controller. The results of pitch response with and without controller have been given in Table 2.

0.00648(s+2.249), the response have been plotted and is compared with the pitch response without controller as shown in Fig. 10. It is found that the transient response of pitch attitude is further improved after adding the PD controller. The results of pitch response with and without controller have been given in Table 2.

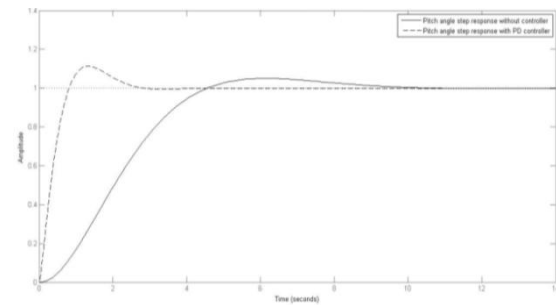


Fig. 10: Comparison of pitch response with and without controller

Table 2: Performance of pitch controller

Specification	Without Controller	With PD Controller
Rise time	2.95 s	0.577 s
Peak time	6 s	1.33 s
Overshoot	5%	11%
Settling time	8.46 s	2.39 s
Steady-state error	zero	zero
Closed-loop stability	stable	stable

4.3. Yaw response

The yaw attitude response with 5% overshoot without controller have peak time of 8.79 s, rise time of 4.2 s, and settling time of 12 s. After adding the PD controller for yaw control having the transfer function $0.22(s+3.5)$, the response have been plotted and is compared with the yaw response without controller as shown in Fig. 11.

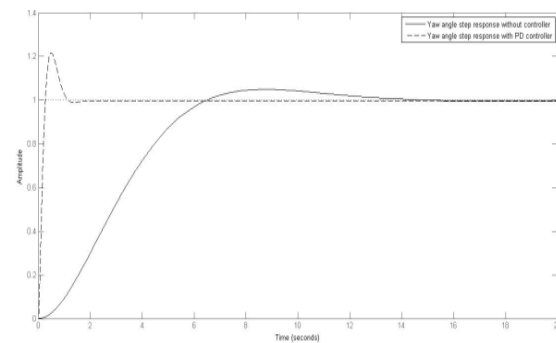


Fig. 11: Comparison of yaw response with and without controller

Table 3: Performance of yaw controller

Specification	Without controller	With PD controller
Rise time	4.2 s	0.193 s
Peak time	8.79 s	0.5 s
Overshoot	5%	20%
Settling time	12 s	1.03 s
Steady-state error	zero	zero
Closed-loop stability	stable	stable

The results of yaw response with and without controller have been given in Table 3. It is found that the transient response of yaw attitude is improved after

adding the PD controller but having an extra overshoot of 15% than the one without controller.

5. Conclusion

The modelling and simulation of quadcopter for attitude control based on classical controllers has been done and analysed using root locus in MATLAB. The transient response graphs have been obtained for the respective transfer functions for roll, pitch, and yaw of the quadcopter. From the results, it is clear that the quadcopter attitude dynamics can be better controlled with classical controllers such as PID. It is noted that, the yaw response produces 20% overshoot in yaw angle but it settles within 1 second. Hence, for controlling the quadcopter in yaw attitude it is advisable to have a yaw rate controller instead of yaw angle control. Once, the model of the quadcopter is obtained or estimated, it is better to design PID controllers to control the quadcopter in noise free environment. In case of adverse conditions, the classical controller could not be a better choice for attitude control of quadcopters. In such circumstances, any non-linear control methods could be suitable for control of rotor type aircrafts. In case of going for PID controllers in adverse environment, the quadcopter model has to be estimated using system identification methods. In summary, the classical controllers have been worked well for control of rotor-type miniature aircrafts.

REFERENCES:

- [1] G.M. Hoffmann, H. Huang, S.L. Waslander and C.J. Tomlin. 2007. Quadrotor helicopter flight dynamics and control: theory and experiment, *Proc. AIAA Guidance, Navigation & Control Conference & Exhibit*. <https://doi.org/10.2514/6.2007-6461>.
- [2] A. Tayebi and S. McGilvray. 2004. Attitude stabilization of a four-rotor aerial robot, *Proc. 43rd IEEE Conf. Decision & Control*, 2, 1216-1221. <https://doi.org/10.1109/CDC.2004.1430207>.
- [3] Z. Benić, P. Piljek and D. Kotarski. 2016. Mathematical modelling of unmanned aerial vehicles with four rotors, *Interdisciplinary Description of Complex Systems*, 14(1), 88-100.
- [4] K.M. Thua and A.I. Gavrilova. 2016. Designing and modeling of quadcopter control system using L1 adaptive control, *Proc. 12th Int. Symp. Intelligent Systems*, 103, 528-535.
- [5] H. Bolandi, M. Rezaei, R. Mohsenipour, H. Nemati, and S.M. Smailzadeh. 2013. Attitude control of a quadrotor with optimized pid controller, *Intelligent Control & Automation*, 4, 335-342. <https://doi.org/10.4236/ica.2013.43039>.
- [6] R. Vijayanandh, S. Senthil kumar M. Senthil kumar and M.B. Sabarish. 2018. Design and fabrication of tilt-hexacopter with image processing for critical applications, *Int. J. Pure & Applied Mathematics*, 118(9), 935-945.
- [7] R. Vijayanandh, S. Mano, M. Dinesh, M. Senthil kumar and G. Rajkumar. 2017. Design, fabrication and simulation of hexacopter for forest surveillance, *APRN J. Engg. & Applied Sci.*, 12(12), 3879-3884.
- [8] K. Nonami, F. Kendoul, S. Suzuki, W. Wang and D. Nakazawa. 2010. *Autonomous flying robots, Unmanned Aerial Vehicles and Micro Aerial Vehicle*, Springer. <https://doi.org/10.1007/978-4-431-53856-1>.
- [9] R. Austin. 2010. *Unmanned Aircraft Systems: UAVs Design, Development and Deployment*, John Wiley & Sons. <https://doi.org/10.1002/9780470664797>.
- [10] N.S. Nise. 2011. *Control Systems Engineering*, John Wiley & Sons.